Electronic Supporting Information

Moisture-sensitive Mechanical Metamaterials with Unusual and Re-programmable Hygroscopic Deformation Modes

Yisong Bai [a], Chuanbao Liu [b], Yang Li [a], Jinxu Li [a], Lijie Qiao [a], Ji Zhou [c], Yang Bai [*a]

[a] Beijing Advanced Innovation Center for Materials Genome Engineering, Institute for Advanced Materials and Technology, University of Science and Technology Beijing, Beijing 100083, China

[b] School of Materials Science and Engineering, University of Science and Technology Beijing, Beijing 100083, China

[c] State Key Laboratory of New Ceramics and Fine Processing, School of Materials Science and Engineering, Tsinghua University, Beijing 100084, China

* To whom correspondence should be addressed: Email: baiy@mater.ustb.edu.cn

Note S1

For the unit cell of the tetrachiral structure, the nodes and the curved strips in the top are taken for example to describe the connection between them due to the rotational symmetry. The center of the nodes (marked with circles) and curved strips (marked with a star) is on the same line in X direction. The nodes are mirror symmetric about the center of the strips. The contour line of the convex side of the strip is directly connected with the left contour line of the node in the left, as shown in Fig. S1a.

For the unit cell of the anti-tetrachiral structure, the nodes in the center and right connected with the curved strips in the right are taken for example to describe the connection due to the rotational symmetry. The contour line of the convex side of the curved strips is exactly connected with the left contour line of the central node, and the contour line of the concave side of the strips is exactly connected with the left contour line of the right node, as shown in Fig. S1b.

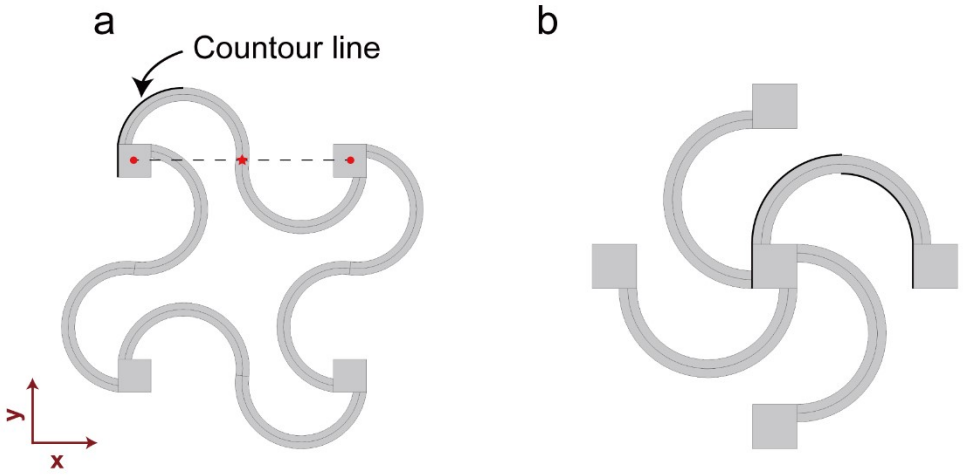

Fig. S1 Illustration of the connection between the curved strips and the nodes.

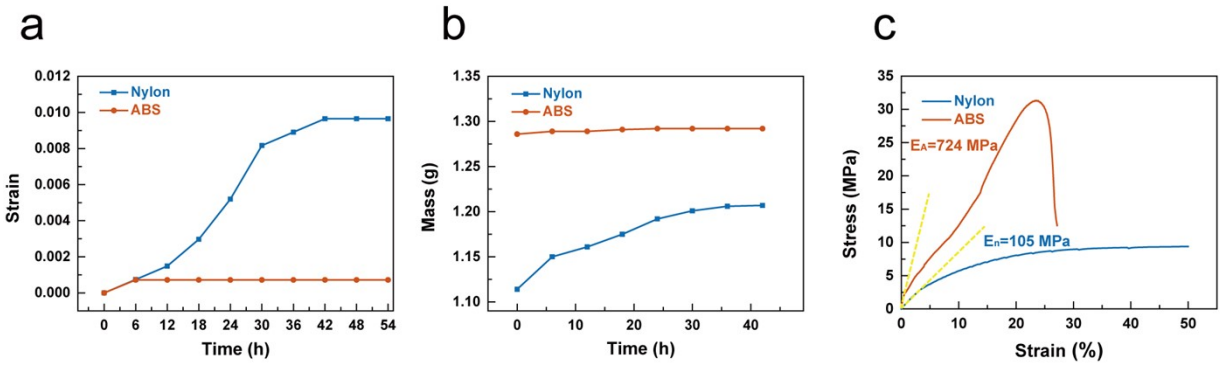

Fig. S2 Measurement of component material properties, all the tested samples were fabricated at 20% RH, 303.15 K. a) Strain-time curves of Nylon and ABS for CHE measuring at 80% RH, 303.15 K. Sample size: 110 mm×2 mm×1 mm. b) Mass-time curves of Nylon and ABS for Young's module measuring at 80% RH, 303.15 K. Sample size: 45 mm×10 mm×3 mm c) Stress-strain curves of Nylon and ABS with saturated moisture state at 80% RH, 303.15 K.

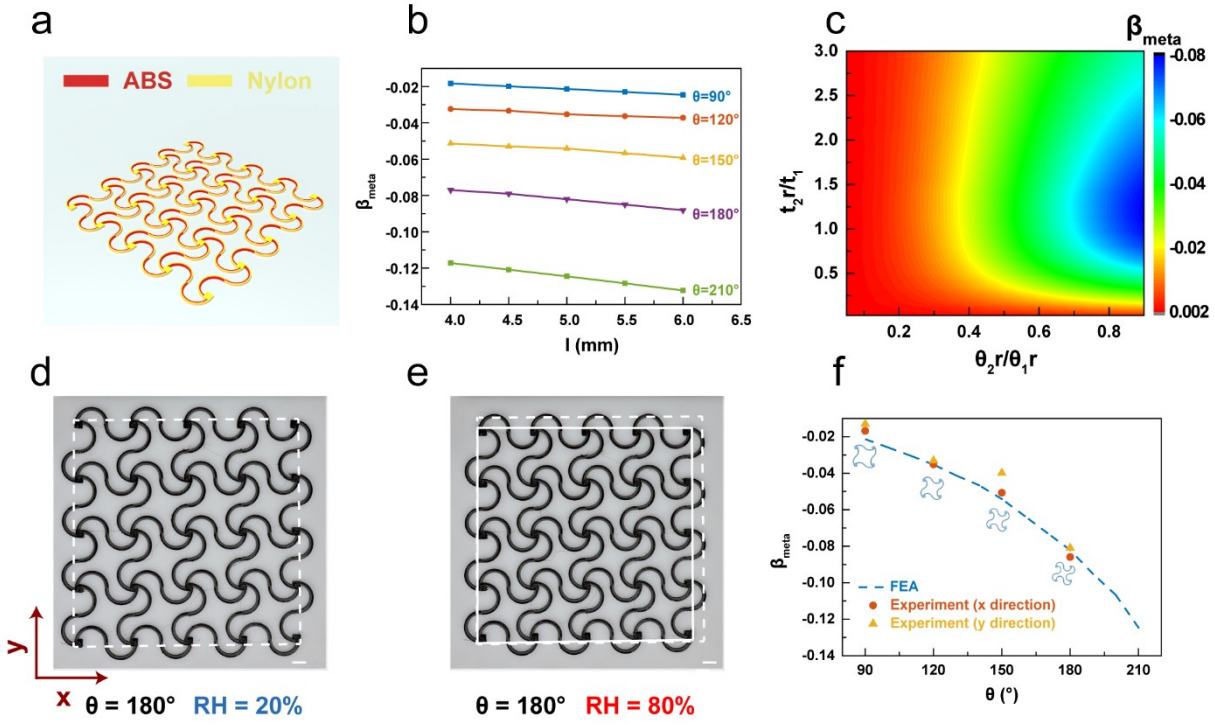

Fig. S3 Isotropic tunable hygroscopic expansion of tetrachiral structure (Outer material = Nylon, Inner material = ABS). a) The schematic illustration of the tetrachiral structure. b, c) The dependence of CHE on node size l, radian θ, arc length ratio $\theta_2 r/\theta_1 r$ and thickness ratio

t_2/t_1. d, e) Optical images of samples at 20% RH (left) and 80% RH (right) with θ =180°. f) FEA and experimental results of the dependence of CHE on radians θ. Scale bars, 10 mm.

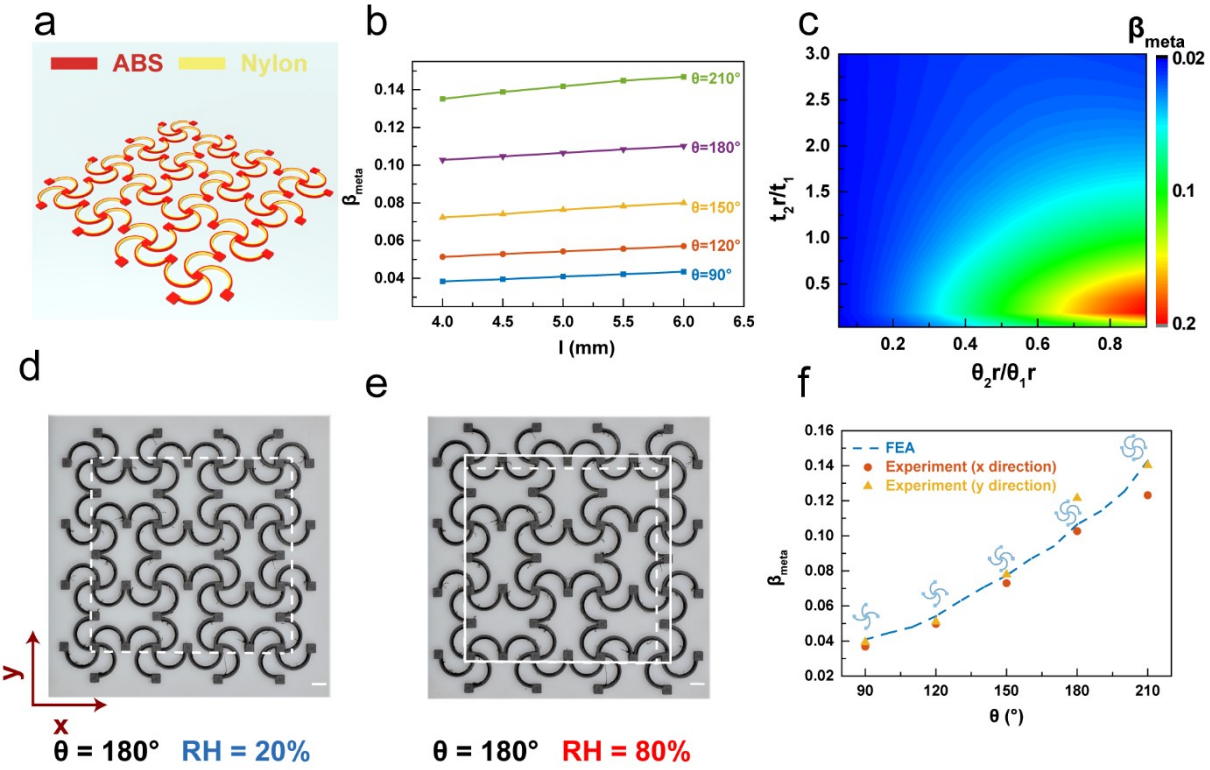

Fig. S4 Isotropic tunable hygroscopic expansion of anti-tetrachrial structure (Outer material = ABS, Inner material = Nylon). a) The schematic illustration of the anti-tetrachiral structure. b, c) The dependence of CHE on node size l, radian θ, arc length ratio $\theta_2 r/\theta_1 r$ and thickness ratio t_2/t_1. d, e) Optical images of samples at 20% RH (left) and 80% RH (right) with θ =180°. f) FEA and experimental results of the dependence of CHE on radians θ. Scale bars, 10 mm.

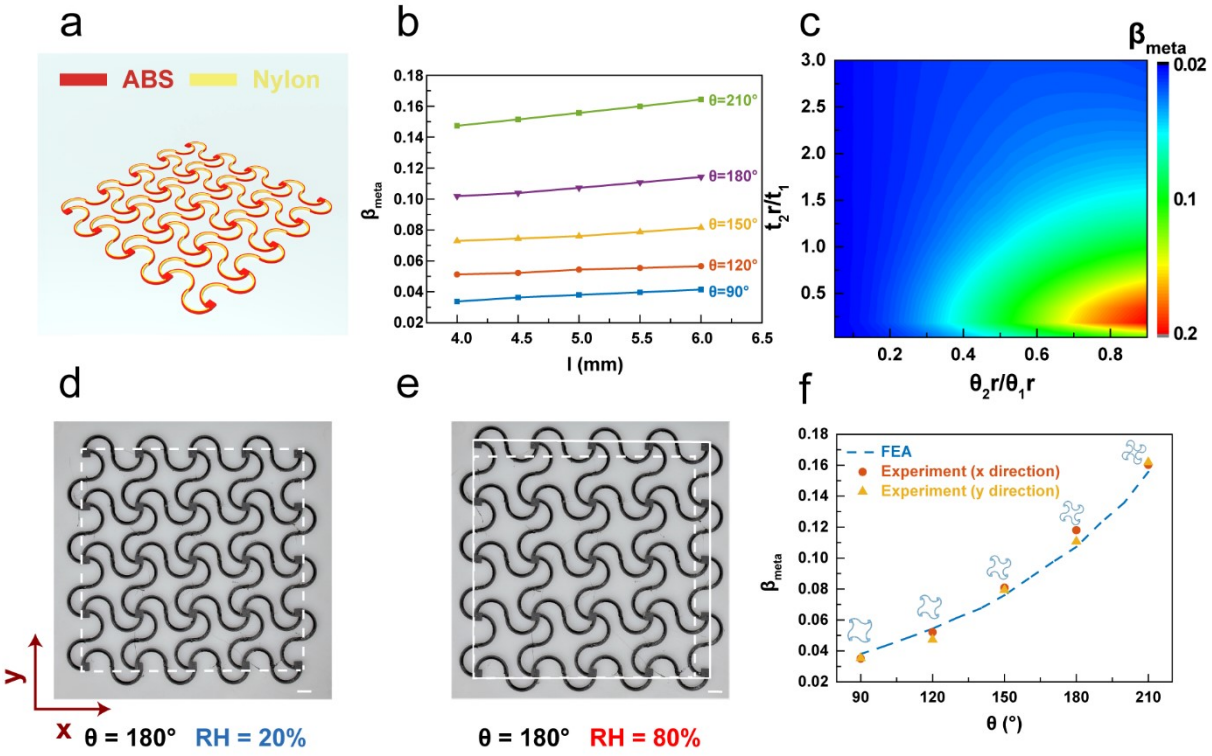

Fig. S5 Isotropic tunable hygroscopic expansion of tetrachiral structure (Outer material = ABS, Inner material = Nylon). a) The schematic illustration of the anti-tetrachiral structure. b, c) The dependence of CHE on node size l, radian θ, arc length ratio $\theta_2 r/\theta_1 r$ and thickness ratio t_2/t_1. d, e) Optical images of samples at 20% RH (left) and 80% RH (right) with θ =180°. f) FEA and experimental results of the dependence of CHE on radians θ. Scale bars, 10 mm.

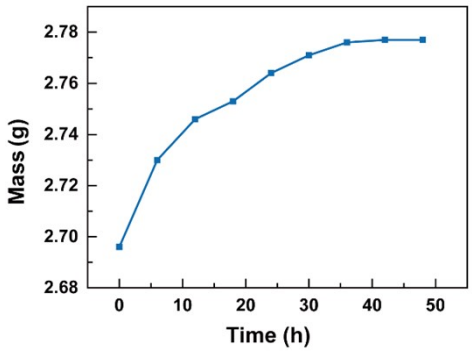

Fig. S6 Mass-time curve for a tetrachiral structure of 2×2 unit cells with θ = 180°, l = 5 mm, a = 20 mm, and $t_1 = t_2$ = 1 mm at 80% RH, 303.15 K, which is fabricated at 20% RH, 303.15 K.

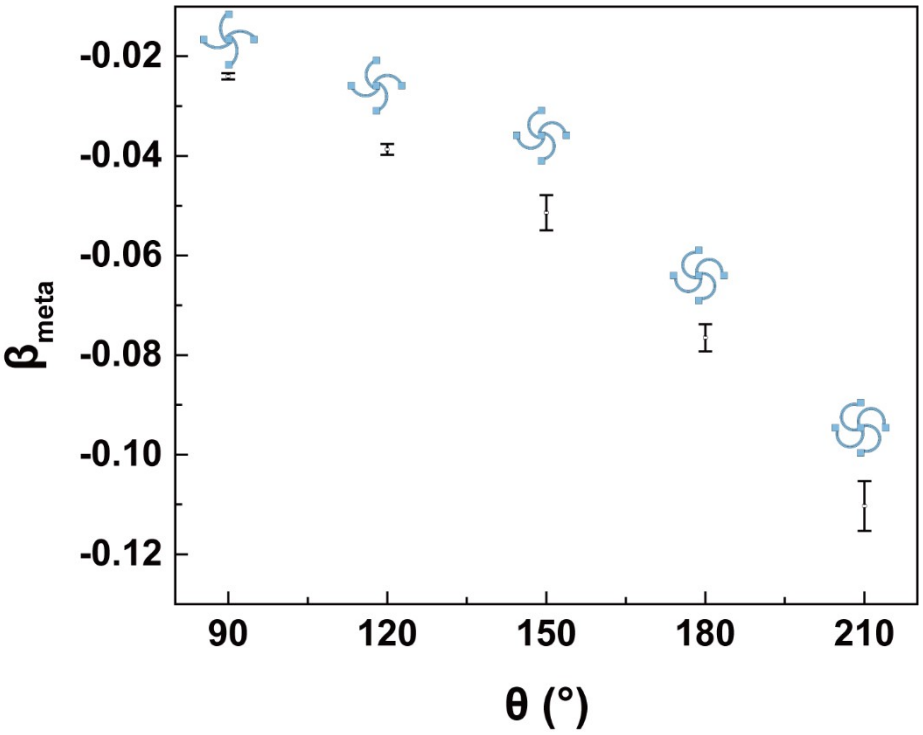

Fig. S7 Experimental results of the dependence of CHE on radians θ.

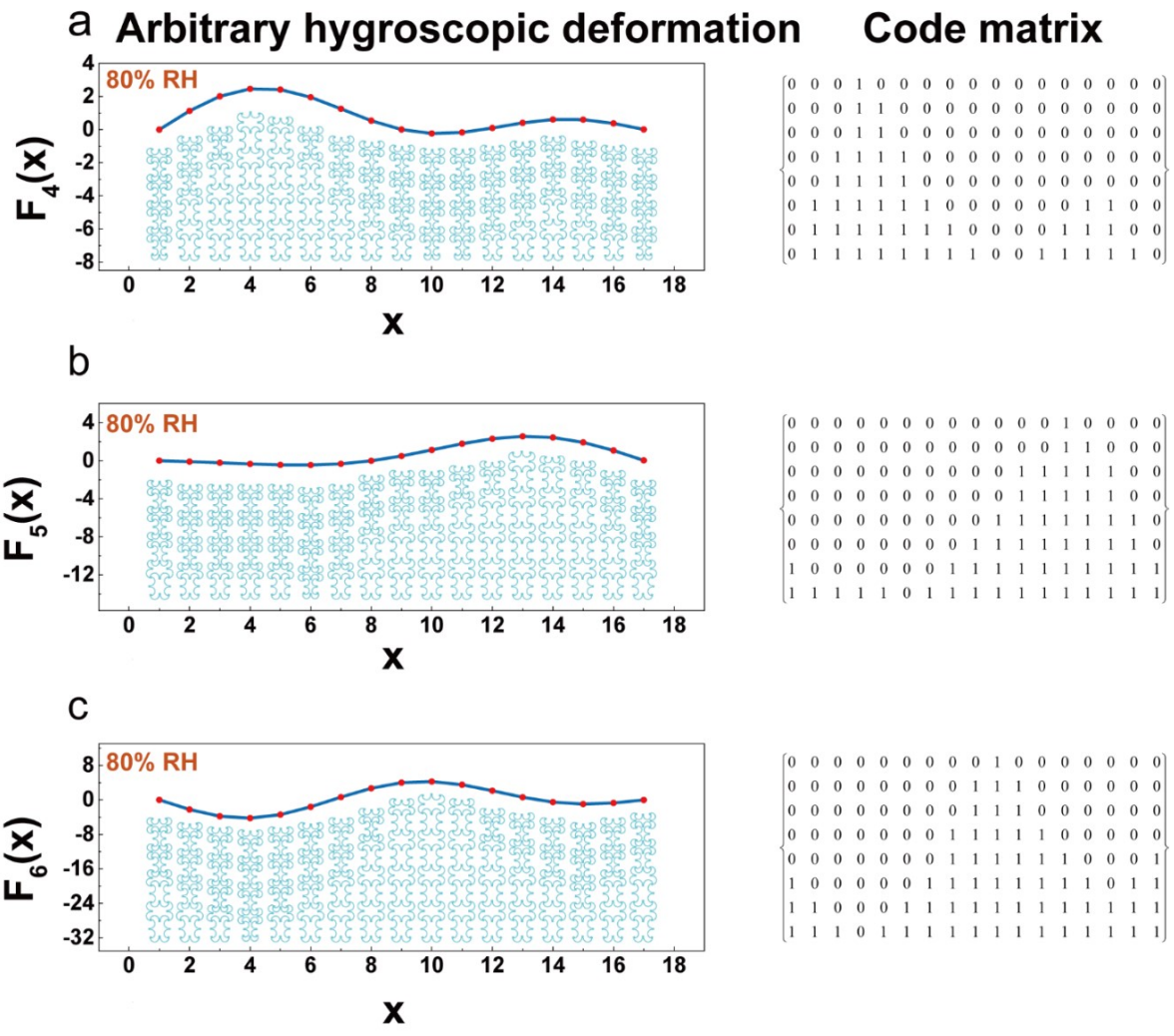

Fig. S8 Arbitrary hygroscopic deformation metamaterials based on modified anti-chiral structure. a-c) The simulated thermal deformation of designed structures fitting the function graph ($F_4(x)$-$F_6(x)$) (left) and corresponding code matrix (right). Scale factor = 3.

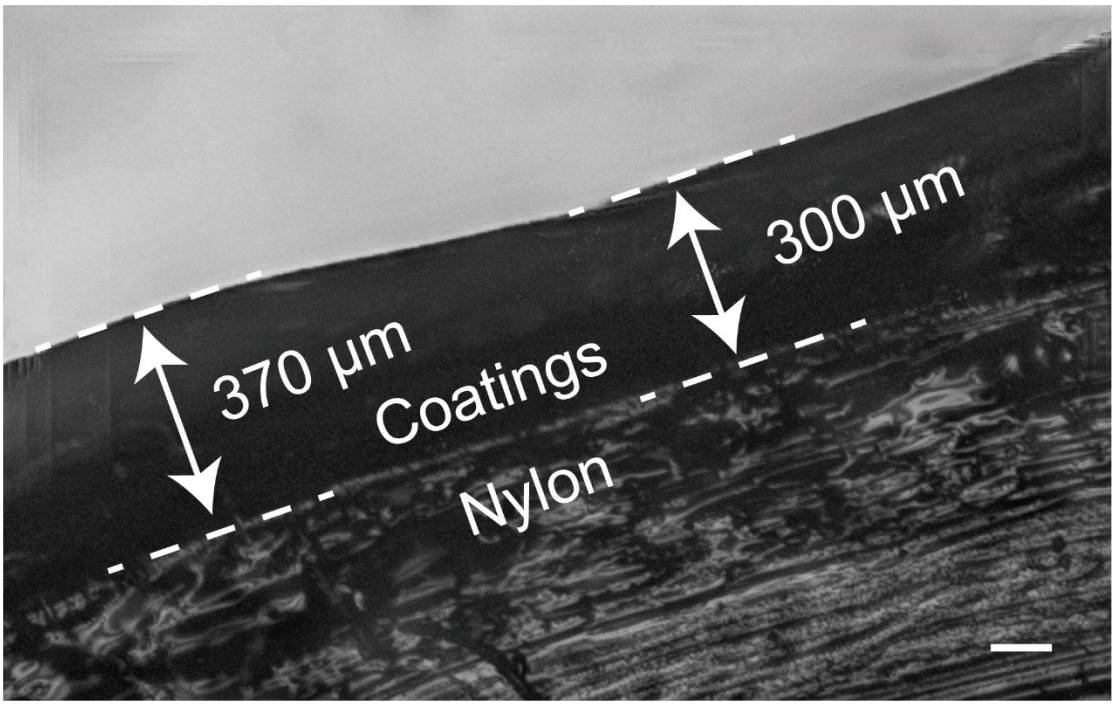

Fig. S9 Local optical image of curved strips with coatings only on the convex side. Scale bar, 100 μm.

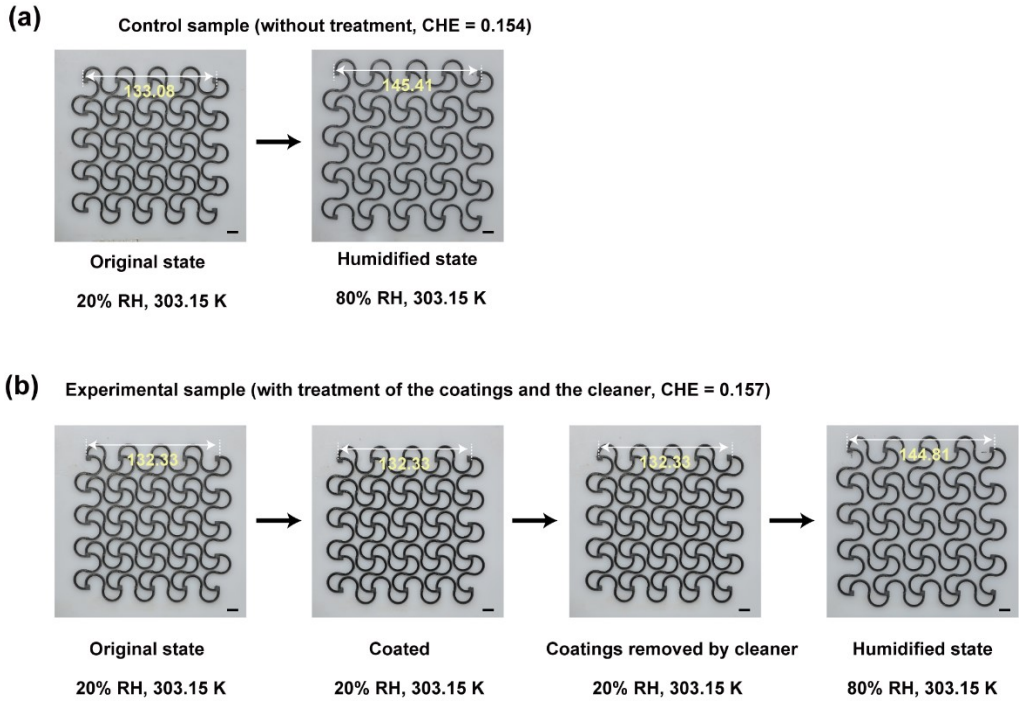

Fig. S10 Effect of the coatings and the cleaner on the hygroscopic deformation of the PHE tetrachiral samples with $\theta = 210°$, $t_1 = t_2 = 1$ mm, $a = 20$ mm and $l = 5$ mm. (a) Optical image of the untreated sample at 20% RH and 80% RH. (b) Optical image of the sample which was painted with coatings and then removed by the cleaner at 20% RH and humidified at 80% RH. The calculated CHE of untreated and treated samples is 0.154 and 0.157, indicating the involvement of the coatings and cleaner has a negligible effect on the hygroscopic properties of the metamaterials. The measurement unit in (a) and (b) is millimeters. Scale bars, 10 mm.

Table S1. Parameters used in the generating functions $F_1(x)$-$F_6(x)$ served as target shape.

	a_1	a_2	a_3	γ
$F_1(x)$	1	0	0	0.196
$F_2(x)$	0	-1	0	0.196
$F_3(x)$	0	0	1	0.196
$F_4(x)$	1	1	1	0.196
$F_5(x)$	1	-1.5	0.5	0.196
$F_6(x)$	1	-2	-3	0.196